

## *In situ* imaging of field emission from individual carbon nanotubes and their structural damage

Zhong L. Wang<sup>a)</sup> and Rui Ping Gao

Center for Nanoscience and Nanotechnology, School of Materials Science and Engineering, Georgia Institute of Technology, Atlanta, Georgia 30332-0245

Walt A. de Heer and P. Poncharal

School of Physics, Georgia Institute of Technology, Atlanta, Georgia 30332-0430

(Received 15 October 2001; accepted for publication 27 November 2001)

Field emission of individual carbon nanotubes was observed by *in situ* transmission electron microscopy. A fluctuation in emission current was due to a variation in distance between the nanotube tip and the counter electrode owing to a “head-shaking” effect of the nanotube during field emission. Strong field-induced structural damage of a nanotube occurs in two ways: a piece-by-piece and segment-by-segment pilling process of the graphitic layers, and a concentric layer-by-layer stripping process. The former is believed owing to a strong electrostatic force, and the latter is likely due to heating produced by emission current that flowed through the most outer graphitic layers. © 2002 American Institute of Physics. [DOI: 10.1063/1.1446994]

Carbon nanotubes have been demonstrated to exhibit superior properties for low-voltage field emission due to their unique geometrical shape.<sup>1,2</sup> Growth of aligned carbon nanotubes<sup>3–5</sup> onto a patterned substrate is a unique feature of carbon nanotubes for applications in advanced technology. Carbon nanotubes,<sup>6</sup> boron carbonitride,<sup>7</sup> and carbon nanobells<sup>8</sup> have been found to exhibit very low turn-on field and superior field emission performance. Carbon nanotubes grow from catalyst particles wherever they are deposited, and one particle usually results in the growth of one nanotube, thus, providing experimental feasibility for designing patterned nanostructures. The field emission properties of carbon nanotubes are usually measured from the aligned nanotubes distributed on a flat substrate, and the theory is based on the Fowler–Nordheim equation,<sup>9</sup> which correlates the emission current density  $J$  and the macroscopic applied electric field  $E$ . The theory applies to the case in which the emission is a collective result of many aligned carbon nanotubes of equal length, identical geometrical shape, and distributed uniformly onto the surface of a large flat substrate. The experimentally measured result is, however, an average over all of the aligned nanotubes that are structurally diverse in diameters, lengths, and helical angles. To properly understand the fundamental physics in carbon nanotube field emission, it is essential to examine the field emission properties of individual nanotubes.

We have developed a technique for measuring the work function at the tips of individual carbon nanotubes using *in situ* transmission electron microscopy (TEM).<sup>10</sup> In this letter, we present *in situ* TEM observation of the electron field emission from individual carbon nanotubes, and the field induced structural damage of multiwalled nanotubes.

The observation was carried out *in situ* in a JEOL 100C TEM (100 kV).<sup>11</sup> A specimen holder was built for applying a voltage across a nanotube and its counter gold electrode. The

detailed experimental setup has been reported elsewhere.<sup>12</sup> The nanotubes to be used for observation are directly imaged in TEM [Fig. 1(a)] and the specimen can be selected so that the emission is mainly from one nanotube. After applying a voltage onto the nanotube, the tip of the nanotube is charged and it bends toward the counter electrode simply due to its long length [Figs. 1(b) and 1(c)]. This length induced bending flexibility is a source of emission current instability for carbon nanotubes.

To observe the electrostatic field distribution due to the charges on a carbon nanotube, we use the beam deflection effect introduced by the electrostatic force. If the nanotube is positively charged [Fig. 2(a)], the electrons passing through

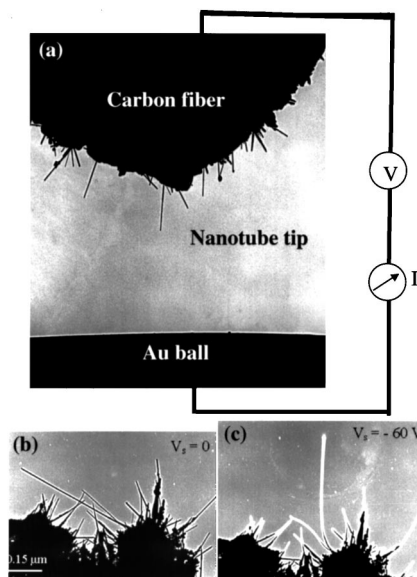


FIG. 1. (a) TEM image of carbon nanotubes and a counterelectrode used for observing the field emission by *in situ* TEM. (b), (c) TEM images of a carbon nanotube at the end of a carbon fiber produced by arc discharge, showing its straight shape and the bent shape prior and post applying a 60 V voltage. The change in nanotube contrast in (c) is due to the buildup of the electrostatic charges at its tip.

<sup>a)</sup>Author to whom correspondence should be addressed; electronic mail: zhong.wang@mse.gatech.edu

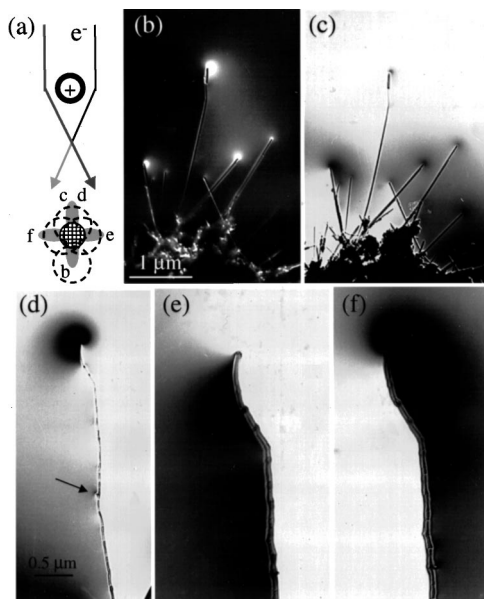


FIG. 2. (a) Schematic diagram showing the deflection of the electron beam passing a positively charged nanotube and the corresponding diffuse scattering around the transmission beam in TEM, where the circles indicate the positions of the objective aperture used for acquiring the images. (b), (c) TEM images of carbon nanotubes produced by arc discharge by positioning the objective aperture at positions b and c, respectively, under an applied voltage of 100 V. The distance from the tip of the nanotube to the counter-electrode was  $\sim 3 \mu\text{m}$ . (e)–(f) TEM images of a carbon nanotube grown by CVD process showing potential distribution at the tip and on both sides of the nanotube. The applied voltage was 120 V. The distance from the tip of the nanotube to the counterelectrode was  $\sim 2.5 \mu\text{m}$ .

the two sides of a nanotube are deflected toward each other due to electrostatic attraction, resulting in a weak diffuse scattering in the electron diffraction pattern around the central transmission beam. By selecting a portion of the diffusely scattered electrons using a small size objective aperture, the field distribution around the nanotube can be revealed. Figures 2(b) and 2(c) are two images of the nanotubes acquired by placing the objective aperture at the b and c positions as indicated in Fig. 2(a), corresponding, respectively, to the dark field and bright field images of the nanotubes that are emitting electrons. The contrast is mostly pronounced near the tips of the nanotubes produced by an arc-discharge technique, confirming the emission of electrons from the tips of the nanotubes, just as expected. The classical definition of turn on field  $E_t = V/d$ , where  $V$  is the applied voltage and  $d$  is the distance from the tip of the field emitter to the surface of the counter electrode, may not be an adequate measurement on the local field at the tips of the carbon nanotube, due to its sharp needle geometry. The experimentally measured turn field for carbon nanotube is as low as  $0.6\text{--}1.0 \text{ V}/\mu\text{m}$ .<sup>13</sup>

For nanotubes produced by chemical vapor deposition (CVD) that usually have more defects and imperfect structures, the field is even appreciable near the defect site, as indicated in Fig. 2(d), although the field is still the maximum near the tip, indicating that the defect region can have electrostatic charge. Figures 2(e) and 2(f) are two images recorded by selecting the electrons deflected to both sides of the nanotube, showing the field distribution around the nanotube. It is apparent that the tube has charge distribution across its entire length to maintain its equal potential surface

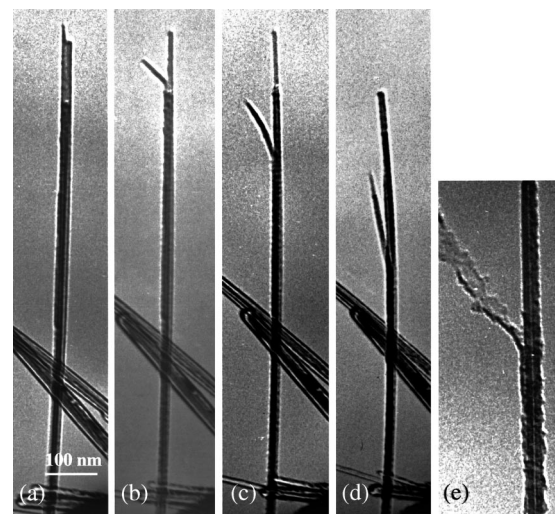


FIG. 3. “Splitting” process in structural damage. (a)–(d) Series of TEM images showing the structural damage of a carbon nanotube during field emission, in which the applied voltage and the emission current are: (a)  $V = 80 \text{ V}$ ,  $I = 10 \mu\text{A}$ , (b)  $V = 90 \text{ V}$ ,  $I = 40 \mu\text{A}$ , (c)  $V = 110 \text{ V}$ ,  $I = 100 \mu\text{A}$ , and (d)  $V = 130 \text{ V}$ ,  $I = 250 \mu\text{A}$ . The distance from the tip of the nanotube to the counter electrode was  $\sim 2 \mu\text{m}$ . (e) Nanotube that is experiencing the splitting of its outer layers during the damage.

(for conductive nanotubes, a case for most of the nanotubes).

A quantitative analysis of the potential field based on these images must consider four important factors: (1) the size and position  $\mathbf{u}_0$  of the objective aperture in reciprocal space,  $D(|\mathbf{u}-\mathbf{u}_0|)$ ; (2) the relative position of the tube in reference to the counter electrode; (3) the beam convergence; and (4) the defocus  $\Delta f$  of the objective lens. The vast difference of the contrast between Figs. 3(e) and 3(f) at the tip of the nanotube is due to beam convergence. If we ignore the beam convergence and ignore the spherical aberration of the objective lens, the image contrast is given in Eq. (1) under the weak-phase-object approximation:

$$I = |D(u_0) + i\sigma V(x,y) \otimes t(x,y) \otimes d_{ap}(x,y)|^2, \quad (1)$$

where  $\sigma = \pi/\lambda U_0$ ,  $U_0$  is the accelerating voltage of the TEM,  $\lambda$  is the electron wavelength,  $V(x,y)$  is the projected potential of the electrostatic field around the tip,  $t(x,y) = \exp[i\pi(x^2+y^2)/\lambda\Delta f]/i\lambda\Delta f$ ,

$$d_{ap}(x,y) = 2\pi \int_0^{u_0} du u J_0(2\pi u \rho),$$

$\rho = [\pi(x^2+y^2)^{1/2}]$ ,  $J_0$  is the Bessel function, and  $\otimes$  is the convolution calculation.

An important phenomenon of our study is the observation of structural damage of a carbon nanotube during field emission under a higher voltage. This study is useful in determining the structural stability of the nanotubes. Figure 3 shows a series of images of a nanotube that was being damaged by an applied voltage. The structural damage is apparent as the applied voltage increases. The damage occurs in such a way that the walls of the nanotubes are split patch-by-patch and segment-by-segment. A closer image of the splitting is shown in Fig. 3(e). This damage process is different from the unraveling process proposed by Rinzier *et al.*,<sup>2</sup> who believed that the nanotubes are damaged following a string-by-string removing of the carbon atoms along the circumference of the graphitic layer.

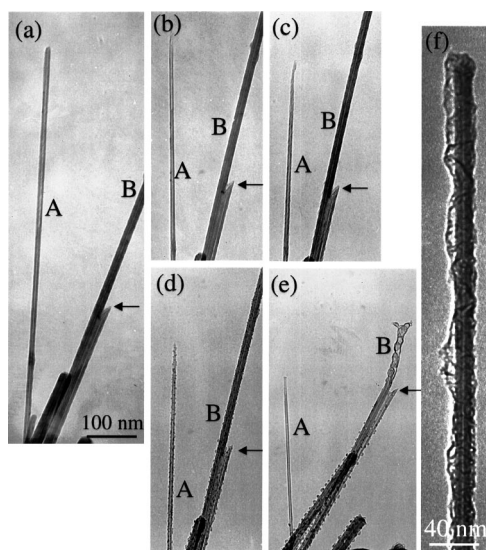


FIG. 4. “Stripping” effect in structural damage. (a)–(e) Series of TEM images showing the structural damage of a carbon nanotube during field emission. The applied voltages were (a)  $V=100$  V, (b)  $V=120$  V, (c)  $V=140$  V, (d)  $V=160$  V, and (e)  $V=200$  V. The distance from the tip of the nanotube to the counterelectrode was  $\sim 4$   $\mu\text{m}$ . (f) A carbon nanotube after passing through a large current, showing the structural damage at the outer graphitic layers, while the internal layers are intact.

Figure 4 shows a “stripping” process of a carbon nanotube under the applied electric field. The diameter and length of the nanotube A decrease as it is being damaged by the field. This is a sharpening process of the multiwalled nanotube. The structure of nanotube B is almost totally damaged by the field and finally becomes a graphitic structure.

The mechanisms of the field-induced damage are believed due to two processes. One, the electrostatic force acting on the tip of the nanotube can split the nanotube piece-by-piece and segment-by-segment, such as the one shown in Fig. 3. The second process is likely due to the local temperature created by the flow of emission current, which may “burn” the nanotube layer-by-layer, resulting in the sharpening process as presented in Fig. 4. The emission current is likely to flow along the nanotube through the most outer graphitic layers.<sup>11</sup> Figure 4(e) shows a TEM image of a carbon nanotube after passing a large current, displaying severe damage near the surface, suggesting that the current flowed through the outer layers. This was first proposed by Frank *et al.*<sup>14</sup> for interpreting the quantum conductance of a multiwalled carbon nanotube at room temperature. This process has recently been used for removing the walls of carbon nanotubes.<sup>15,16</sup>

It was reported by Rinzler *et al.*<sup>2</sup> that the current emitted by nanotubes fluctuates almost randomly as a function of time at the time scale of a couple of seconds, and this phenomenon was interpreted owing to a unraveling process of the carbon atom ring. Through *in situ* TEM observation, we found that the fluctuation in emission current is due to a

“head-shaking” effect of the nanotube while emitting electrons. As previously shown in Fig. 1(c), the nanotube bends toward the counter electrode at an applied voltage. The emission of electrons from a nanotube is likely to be a “ballistic” emission process in which the electrons are emitted as groups, although each emission can release many electrons. When the nanotube is fully charged prior to emission, the distance between the nanotube tip and the counter electrode is the smallest due to the strongest electrostatic attraction; as soon as the electrons are emitted as a group, the electrostatic force between the nanotube and the electrode drops slightly, resulting in the recovery of the nanotube shape and a larger distance from the electrode. The head shaking of the nanotube due to “ballistic” emission results in a variation in the distance of its tip from the electrode, thus, leads to a fluctuation in the emission current. This may also account for the blinking of emission current from carbon nanotubes. The ballistic emission is possible because the small size of a nanotube can only hold a small amount of electrons at its tip. A rough estimation indicates that losing one electron at the tip can change the tip potential by  $\sim 0.15$  V for a 20 nm diameter nanotube. The head shaking is a result of its large aspect ratio that leads to body swing during field emission.

The authors are grateful to the support from U.S. NSF Grant No. DMR-9733160 and the NSF of China, the Georgia Tech Electron Microscopy Center for providing the research facility.

- <sup>1</sup>W. A. De Heer, W. S. Bacsá, A. Chatelain, T. Gerfin, R. Humphreybaker, L. Forró, and D. Ugarte, *Science* **268**, 845 (1995).
- <sup>2</sup>A. G. Rinzler, J. H. Hafner, P. Nikolaev, L. Lou, S. G. Kim, D. Tomanek, P. Nordlander, D. T. Colbert, and R. E. Smalley, *Science* **269**, 1550 (1995).
- <sup>3</sup>W. Z. Li, S. S. Xie, L. X. Qian, B. H. Chang, B. S. Zou, W. Y. Zhou, R. A. Zhao, and G. Wang, *Science* **274**, 1701 (1996).
- <sup>4</sup>Z. F. Ren, Z. P. Huang, J. H. Xu, P. B. Wang, M. P. Siegal, and P. N. Provencio, *Science* **282**, 1105 (1998).
- <sup>5</sup>S. Fan, M. G. Chapline, N. R. Franklin, T. W. Tombler, A. M. Cassell, and H. Dai, *Science* **283**, 512 (1999).
- <sup>6</sup>Z. W. Pan, F. C. K. Au, H. L. Lai, W. Y. Zhou, L. F. Sun, Z. Q. Liu, D. S. Tang, C. S. Lee, S. T. Lee, and S. S. Xie, *J. Phys. Chem. B* **105**, 1519 (2001).
- <sup>7</sup>X. D. Bai, J. D. Guo, J. Yu, E. G. Wang, Jun Yuan, and W. Zhuo, *Appl. Phys. Lett.* **76**, 2624 (2000).
- <sup>8</sup>X. C. Ma, E. G. Wang, W. Zhou, D. A. Jefferson, J. Chen, S. Z. Deng, N. S. Xu, and J. Yuan, *Appl. Phys. Lett.* **75**, 3105 (1999).
- <sup>9</sup>R. H. Fowler and L. W. Nordheim, *Proc. R. Soc. London, Ser. A* **119**, 173 (1928).
- <sup>10</sup>R. P. Gao, Z. W. Pan, and Z. L. Wang, *Appl. Phys. Lett.* **78**, 1757 (2001).
- <sup>11</sup>P. Poncharal, Z. L. Wang, D. Ugarte, and W. A. de Heer, *Science* **283**, 1513 (1999).
- <sup>12</sup>Z. L. Wang, P. Poncharal, and W. A. De Heer, *Pure Appl. Chem.* **72**, 209 (2000).
- <sup>13</sup>Z. W. Pan, F. C. K. Au, H. L. Lai, W. Y. Zhou, L. F. Sun, Z. Q. Liu, D. S. Tang, C. S. Lee, S. T. Lee, and S. S. Xie, *J. Phys. Chem. B* (in press).
- <sup>14</sup>S. Frank, P. Poncharal, Z. L. Wang, and W. A. De Heer, *Science* **280**, 1744 (1998).
- <sup>15</sup>J. Cumings, P. G. Collins, and A. Zettle, *Nature (London)* **406**, 586 (2000).
- <sup>16</sup>P. G. Collins and P. Avouris, *Nanoletters* **1**, 453 (2001).